Collective dipole oscillations in small silver clusters embedded in rare-gas matrices

S. Fedrigo, W. Harbich, and J. Buttet
Institut de Physique Expérimentale, Ecole Polytechnique Federale de Lausanne, PHB-Ecublens, CH-1015 Lausanne, Switzerland
(Received 14 September 1992; revised manuscript received 11 January 1993)

The optical-absorption spectra of small mass-selected Ag_N clusters ($N=2$–21) embedded in solid argon are measured in the energy range 2.5–6.2 eV. Investigation of a continuous range of cluster sizes reveals the size development of the photoabsorption behavior. The main features of the spectra are in agreement with predictions based on the Nilsson-Clemenger shell model. The measured photoabsorption cross sections are consistent with a sum-rule calculation involving only s electrons. In addition, the medium influence on the spectra is studied by changing the matrix gas from argon to krypton and xenon for the cluster sizes $N=7$, 11, 15, and 21.

I. INTRODUCTION

One of the most representative physical phenomena characterizing a bulk metal is the collective excitation of valence electrons, i.e., the plasmon resonance. How many electrons are required in order that a cluster exhibit such a collective behavior is an interesting question, which can shed light on the evolution of the metallic character of a cluster as a function of size. For more than 20 years, electronic size effects have been studied[1–4] by inspecting the optical properties of small particles of diameter of the order of 100 Å or smaller. Classical electrodynamic calculations[5] (Mie) indicate that the strong absorption peak observed in small particles may be attributed to the excitation of surface plasmons (dipolar resonance). The experimental peak position is in good agreement with the Mie prediction taking into account the dielectric constants of the bulk metal and of the surrounding medium. The width of the spectra has been explained by introducing a term varying linearly with the inverse diameter of the particle.

More recently the photoabsorption spectra of small size-selected clusters have been obtained using the molecular-beam photodepletion technique. The authors of Ref. 6 studied the photoabsorption spectra of small sodium clusters ($N=3$–40); they estimate that a transition from molecularlike to collective electronic excitations occurs in the size range $N=3$–5. Configuration-interaction (CI) calculations[7] have shown, however, that the experimental spectra for small clusters ($N\leq 8$) can be interpreted in terms of a group of molecular transitions which are concentrated in a very narrow energy range. Photoabsorption spectra of small clusters in a beam have since been obtained for the alkali metals Na,[8] Li,[9] K,[10,11] and Cs;[12] they have been discussed predominantly in terms of collective excitations. In the case of charged K clusters, the plasmon resonance has been observed for clusters of sizes as large as $N=900$ atoms.[13] In the case of alkali-metal clusters the simple Drude model for the dielectric constant predicts a resonance at the frequency $\omega_r^2=\omega_p^2/3$. With respect to this value, the measurements show a small redshift, which can be explained by taking into account the spilling out of the valence electrons beyond the positive-ion region. A more detailed analysis indicates that effective-mass corrections and core-polarizability effects must be taken into account for Li,[14] K, and, possibly, Na clusters. Most absorption spectra show one main peak, while some spectra exhibit two principal absorption peaks; in rare cases it is possible to distinguish a triple-peak feature. This has been explained[15] by introducing distortions of the spherical shape (one peak) into a spheroidal (two peaks) or an ellipsoidal (three peaks) shape.

In the simplest calculations it is assumed that the valence electrons can be described as moving in an effective one-electron potential,[15] which is approximated, e.g., by an anharmonic oscillator. In more-refined calculations the electronic response of the clusters has been calculated in the spherical (or spheroidal) jellium model using the time-dependent local-density approximation[16] (TDLDA) or the random-phase approximation[17] (RPA). The calculations predict surface plasmons plus electron-hole excitations and, in the case of Na_{20}, a fragmentation of the resonance peak due to the coupling between the collective mode and a one-electron excitation. The Na_{20} spectrum[8] has been interpreted in this way. The Thomas-Fermi statistical method[18] has also been used to describe the photoabsorption of small metal clusters. In the case of alkali-metal clusters with a small number of atoms it is possible to use sophisticated quantum calculations. The absorption spectra of Na_4 and Na_8 (Ref. 19) have been, for example, calculated by CI techniques for different isomers; the calculated transitions are in excellent agreement with the observed spectra and allow one to distinguish between different isomers.

The optical properties of noble metals are more difficult to interpret, and in a way, more interesting than those of the alkali metals, since the effect of the interband transitions due to the d electrons must be considered. For example, in the case of silver, which has a strong absorption peak, the observed bulk plasmon energy (3.78 eV) is much smaller than the Drude model value (9 eV) due to this effect. A crucial question is thus to know how the d electrons affect the optical properties as a function of the cluster size.

The optical properties of embedded silver clusters of

 ©1993 The American Physical Society

sizes of the order of 100 Å have been reviewed[1] and a controversy about the position of the plasmon resonance as a function of the mean size of the particle has developed. This question is now settled; in particular, Charlé, Schulze, and Winter[20] have obtained absorption spectra of silver clusters in an argon matrix with mean numbers of atoms varying between 150 and 3×10^4. They observed plasmon resonances which are blueshifted with respect to the large particle value when decreasing the particle size. Recently Meiwes-Broer and co-workers[21] measured the absorption of size-selected charged clusters of silver containing up to 21 atoms by the photodepletion technique. They have found broad absorption bands (width ≈ 0.6 eV) interpreted as surface plasmon resonances.

In this paper we report on the optical absorption of small mass-selected silver clusters frozen in rare-gas matrices. Spectra of particles in argon are presented for a majority of sizes comprised of between 2 and 21 atoms per cluster. In order to study the effect of the matrix gas, sizes, 7, 11, 15, and 21 are also studied in krypton and xenon matrices. The well-resolved spectra show, depending on the size, the one-, two-, and three-peak structures predicted by a simple model. We discuss the influence of the cluster-matrix interaction and present a model, suggested by Meiwes-Brower,[22] which takes into account the size dependence of the *d*-electron contribution, to link our results with the larger cluster measurements of Charlé, Schulze, and Winter.[20]

II. EXPERIMENT

The experimental setup is shown in Fig. 1. It has been described in detail previously.[23] Briefly, silver ions are sputtered from a metal target using an intense, high-energy (typically 7 mA, 23 keV) xenon-ion beam. The cluster cations are extracted at 90° to the primary beam, focused into an energy filter, and mass selected by a quadrupole mass filter. Cluster ions are decelerated before deposition to typically 30 eV and then codeposited with the matrix gas on a cold (10 K) CaF_2 window cooled by a closed-cycle refrigerator. The deposition window is largely enclosed in a conducting cage, which serves to decelerate the cluster ions, whose deposition energy is adjusted by changing the potential difference applied between the silver sputtering target and the cage. Typical measured currents for silver cations are Ag_5 (3.7 nA), Ag_{11} (2.2 nA), and Ag_{21} (1.8 nA) at 30-eV kinetic energy. The ions were neutralized by a charge cloud of electrons maintained in the proximity of the CaF_2 window.

Matrix samples were studied *in situ* using both excitation and absorption spectroscopy. The light from either a deuterium or a tungsten/halogen lamp was dispersed by a monochromator. In excitation, the light was focused onto the sample [Fig. 2(a)]. The emitted photons were collected at 90°, filtered (in most instances) by a long pass filter, focused into a second monochromator (which was operated in zeroth order), and then detected by a photomultiplier tube.

In absorption, the light coming from the first monochromator was made parallel in order to illuminate the CaF_2 window. An image of the sample was formed on a chopper which splits the light beam into two halves, one passing through the particles plus matrix (the signal), the other passing only through the matrix, thus serving as a reference beam [Fig. 2(b)]. To increase the sensitivity, a diaphragm mounted near the chopper eliminates photons which come from the low-density part of the sample [corresponding to the circle in Fig. 2(b)]. The light was then detected by a photomultiplier tube using pulse counting techniques. Typical count rates of 10 MHz were used without significant pileup. The spectra were recorded as the ratio of the reference beam count rate to the signal beam count rate. This system proved very useful, particularly in the UV range of the spectrum, where extinction due to scattering from rare-gas microcrystallites becomes important.

By comparing the excitation spectra of atoms, dimers,

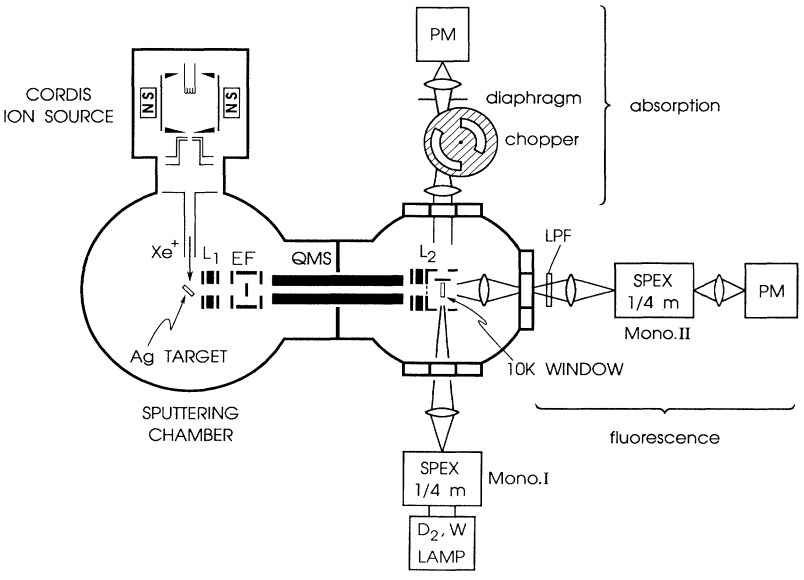

FIG. 1. Experimental setup. Silver cluster cations, sputtered by a xenon-ion beam, are extracted by a lens ($L1$) and focused in an energy filter (EF). They are then size selected by a quadrupole mass filter (QMS) and decelerated by the second lens ($L2$), which directs them to the cooled CaF_2 window. The cryostat can rotate.

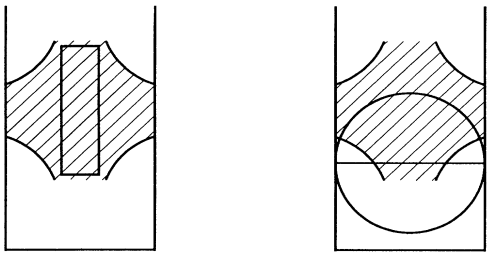

a) b)

FIG. 2. CaF_2 window supporting the particles (dashed area). The strange shape of the sample is due to the quadrupole mass filter. (a) In fluorescence the light coming from the monochromator (Mono. I in Fig. 1) is focused into the sample center. The rectangle corresponds to the image of the monochromator slit. (b) In absorption the parallel light beam illuminates the entire window. The image of the sample is then separated into two parts by a chopper (horizontal line). A photomultiplier collects the light via a diaphragm (circle) which cuts the undesirable light.

and trimers resulting from the fragmentation of the deposited particles with the spectra obtained by direct deposition of Ag_1, Ag_2, and Ag_3, we can estimate the fragmentation rate. We find that in argon matrices, the number of small clusters (one to three atoms) in the sample due to fragmentation is smaller than 20% of the number of deposited cations, at around 30-eV kinetic energy. The fragmentation in Kr and Xe matrices is generally larger. These results are discussed below. Because our matrices are highly dilute (higher than 10^5:1) no aggregation occurs. This means that the observed features must be attributed to deposited species or their fragments, but not to larger-sized clusters.

III. RESULTS

Figure 3 shows the absorption spectra of Ag_N ($N=2-21$, except $N=4$, 6, 10, 12, and 14) in solid argon at 10 K. The deposition energies were 30 eV except for Ag_2 and Ag_3, which were deposited at 20 eV in order to decrease the fragmentation. To get a sufficient current of Ag_8, it was necessary to increase the deposition energy to 50 eV. Typically, about 10^{14} particles were deposited for each cluster size. The spectral region which has been examined extends from 600 to 200 nm (2.1–6.2 eV). Depending on the thickness of the matrix and on the cleanliness of the substrate before the deposition, the background can increase considerably in the region 5–6 eV. Most of the spectra shown are background corrected. The background was fitted by a second degree polynomial and then subtracted from the signal.

A. Atoms, dimers, and trimers

The dimer spectrum shows three main absorption bands centered at 4.75, 3.2, and 2.8 eV assigned to Ag_2

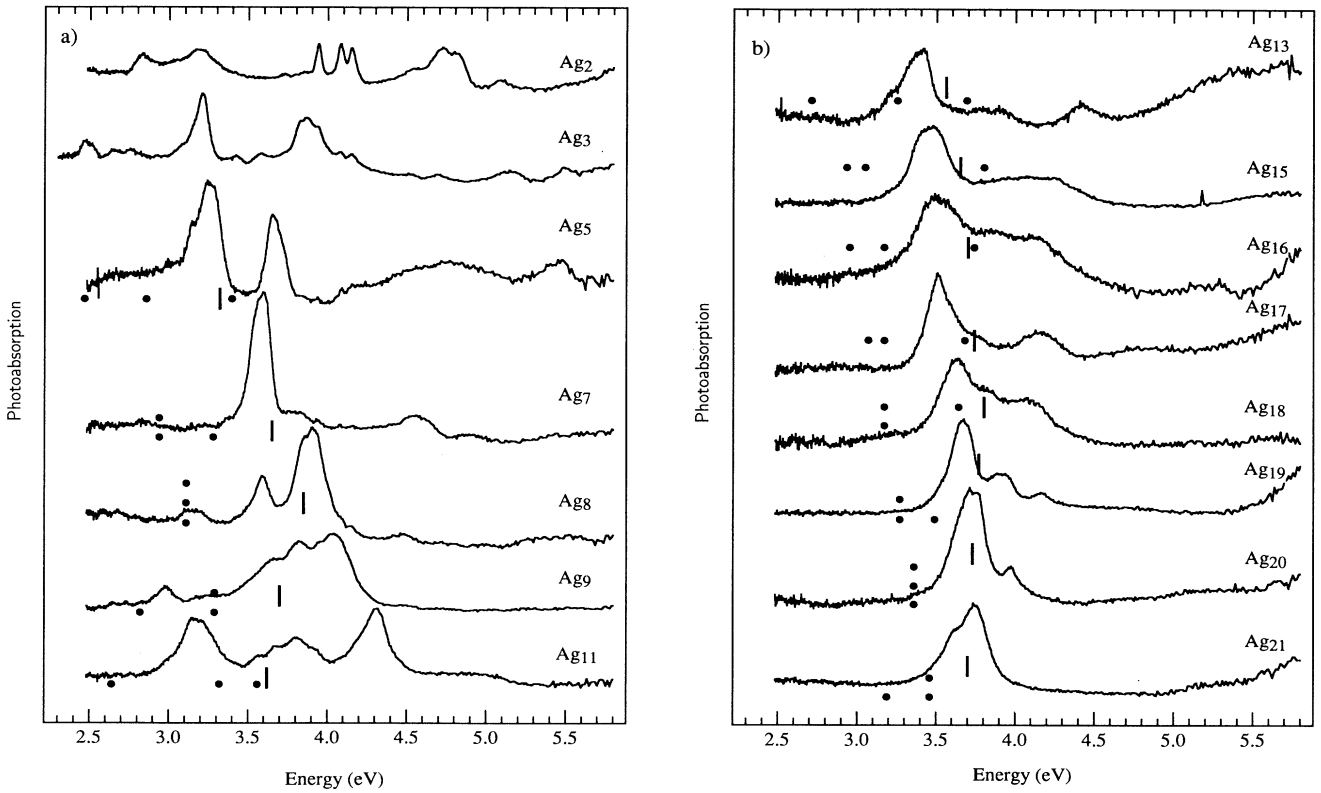

FIG. 3. Photoabsorption spectra of small silver clusters in solid argon for sizes $N=2-11$ (a) and sizes $N=13-21$ (b). In order to reveal the structure of the spectra, the vertical scales are arbitrary. The bars indicate the mean absorption energy for each size and the points correspond to the absorption energies calculated with the Mie-Drude-spillout three-axes model using a spillout of 0.75 Å (see the text).

and a strong atom signal (three peaks at 4.16, 4.08, and 3.94 eV) arising from fragmentation. The trimer spectrum shows two principal absorption bands (3.86 and 3.21 eV) plus a smaller one at 2.49 eV which are all assigned to Ag_3. The atom and dimer results are in good agreement with previous work on silver clusters embedded in argon,[24] while the trimer spectrum confirms our excitation and fluorescence measurements for Ag_3 in krypton[23] and argon[25] matrices. These spectra indicate that the fragmentation in trimer deposition does not much affect the features of interest (see the small response of Ag_1 and Ag_2 in the trimer spectrum).

B. Five to 21 atom clusters

The spectra for Ag_5 to Ag_{21} show one to three principal absorption peaks in the energy range between 3 and 4.5 eV. No absorption was detected further to the red. Except for Ag_8, every absorption peak is assigned to the deposited particles. We used three different techniques to determine whether or not a particular peak is due to the original cluster: (1) the presence of fragments can be detected by comparing a given size absorption spectrum with that of a smaller size, (2) the excitation spectroscopy gives information about the number of atoms, dimers, and trimers contained in the sample, and (3) varying the kinetic energy of the deposited clusters modifies the fragmentation ratio, which induces a variation in the absorption peak intensities. Using these three methods, the second peak (at 3.6 eV) in the Ag_8 spectrum is assigned to the heptamer.

Ag_5 to Ag_{11} were already described in detail previously.[26] Table I summarizes the center and the width [full width at half maximum (FWHM)] of all absorption peaks found by applying a multi-Gaussian fit. A fit with Lorentzian shape has been tried as well but the quality of the fit was clearly inferior to the Gaussian one. The typical width of all absorption peaks is 0.2 eV. The mean absorption energies, defined in the usual way, i.e.,

$$\langle \hbar\omega \rangle = \hbar \frac{\int \sigma(\omega)\omega \, d\omega}{\int \sigma(\omega) d\omega} ,$$

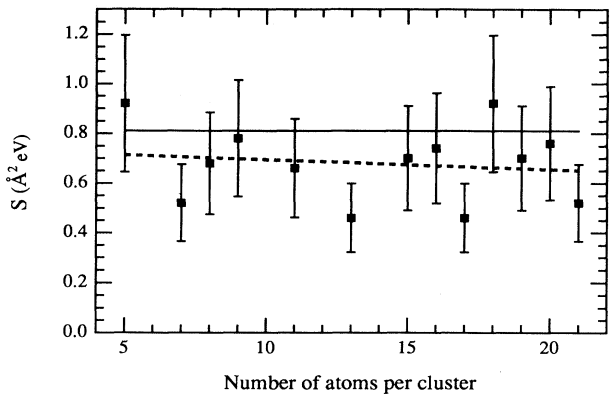

FIG. 4. Absorption cross section per s electron as a function of cluster size. The dashed line corresponds to a linear fit and the solid one to the value given by the sum rule involving only s electrons and taking into account the effect of the matrix.

where $\sigma(\omega)$ is the cross section at frequency ω, are also listed in Table I. They are indicated by vertical bars in Fig. 3. The total width (D) of the complete spectrum evolves continuously with size. It increases from Ag_7 ($D = 0.15$ eV) to Ag_{11-13} ($D = 1.5$ eV) and then decreases towards Ag_{21} ($D = 0.3$ eV).

The determination of the absorption cross section is difficult in these experiments because the deposition efficiency (i.e., the ratio between the number of clusters embedded in the matrix and the number of deposited particles, estimated by measurement of the deposition current) cannot be controlled precisely. It was estimated to be 50% in the case of atom deposition[27] and assumed to be the same for depositions of larger-sized clusters. By integrating the absorption over the whole spectrum we find a mean value of 0.72 eV Å^2 per valence electron (s electron). This value is in good agreement with the gas-phase measurements of Tiggesbäumker *et al.*[21] This implies that on the average 88% of the total oscillator strength due to the s electrons, as determined by the dipole sum rule,[28]

TABLE I. Position energies (eV) and widths Δ (eV) of the measured absorption peaks for a given cluster size. $\langle \hbar\omega \rangle$ is the mean energy (see text) of the absorption spectrum and D its total width.

N	$\hbar\omega_1$	Δ_1	$\hbar\omega_2$	Δ_2	$\hbar\omega_3$	Δ_3	$\langle \hbar\omega \rangle$	D
5	3.27	0.17	3.67	0.12			3.32	0.56
7	3.58	0.11	4.56	0.21			3.65	
8	3.16	0.12	3.89	0.21			3.85	0.90
9	3.68	0.18	3.82	0.18	4.04	0.18	3.70	
11	3.18	0.25	3.78	0.42	4.29	0.22	3.62	1.30
13	3.38	0.19	3.83	0.27	4.42	0.20	3.56	1.30
15	3.46	0.24	3.92	0.25	4.22	0.25	3.65	1.05
16	3.51	0.30	3.88	0.27	4.18	0.27	3.70	1.00
17	3.52	0.22	4.14	0.23			3.74	0.85
18	3.62	0.27	4.04	0.27			3.80	0.75
19	3.68	0.17	3.91	0.18	4.15	0.17	3.77	0.65
20	3.70	0.20	3.97	0.12			3.73	0.45
21	3.56	0.17	3.74	0.19			3.67	0.35

$$\int_{\omega=0}^{\infty} \sigma(\omega) d\omega = CN \ ,$$

is exhausted by the measured transitions. Figure 4 displays the integral absorption cross section per s electron for each cluster size. The large error bars are mainly due to the uncertainties in the deposition efficiency. Under the same deposition conditions for each size (which is the case in our experiment), this error is probably systematic, meaning that the integrated absorption is overestimated or underestimated in the same way for all sizes.

IV. MODELS

Most of the simple models are based on the Mie theory.[5] The interaction of light with a spherical particle embedded in a medium is studied in the framework of classical optics, assuming that the particle and the medium are continuous, homogeneous, and characterized by their dielectric function. When the cluster diameter is much smaller than the wavelength of the incident light, the absorption cross section in the dipolar approximation is derived as

$$\sigma(\omega) = 9 \frac{V}{c} \epsilon_m^{3/2} \frac{\omega \epsilon''}{(\epsilon' + 2\epsilon_m)^2 + \epsilon''^2} \ , \tag{1}$$

where V is the particle volume, c is the speed of light in vacuum, $\epsilon(\omega) = \epsilon' + i\epsilon''$ is the complex dielectric function of the cluster material, and ϵ_m is the dielectric function of the embedding medium (supposed to be real). Assuming that ϵ'' is constant in the studied energy range (which is realistic in most cases) we obtain the Mie resonance condition,

$$\epsilon'(\omega) + 2\epsilon_m = 0 \ . \tag{2}$$

Using the Drude model for the dielectric function of the cluster material, Eq. (2) yields the collective excitation frequency

$$\omega_{\text{res}} = \frac{\omega_p}{(1+2\epsilon_m)^{1/2}} \ , \tag{3}$$

where ω_p is the Drude plasmon frequency which is proportional to the inverse of the square root of the static polarizability. For randomly oriented ellipsoidal particles, the last three expressions become

$$\sigma(\omega) = \frac{V}{3c} \epsilon_m^{3/2} \sum_{i=1}^{3} \frac{1}{L_i^2} \frac{\omega \epsilon''}{[\epsilon' + \epsilon_m (L_i^{-1} - 1)]^2 + \epsilon''^2} \ , \tag{4}$$

$$\epsilon'(\omega) + (L_i^{-1} - 1)\epsilon_m = 0 \ , \tag{5}$$

$$\omega_{\text{res}} = \frac{\omega_p}{[1 + \epsilon_m (L_i^{-1} - 1)]^{1/2}} \ , \tag{6}$$

where L_i are geometric factors[29] related to the depolarization effect. They are equal to $\frac{1}{3}$ in the spherical case. Knowing the principal axes of the cluster, this model predicts three resonance frequencies (degenerated or not) with the same intensity (in the first order of approximation).

Following the Nilsson-Clemenger model,[15] which successfully reproduces several cluster properties, the lengths of the particle axes (X_0, Y_0, and Z_0) are determined by minimizing the energy of the three-dimensional harmonic oscillator with independent valence electrons. The volume of the particle is constrained by $X_0 Y_0 Z_0 = R^3$ where the classical radius R of a sphere containing N conduction electrons is defined by the relation $R = N^{1/3} r_s$ (where r_s is the Wigner-Seitz radius). The energy scale of the oscillator is found by equating the mean square radius of the electronic cloud with the corresponding value for a uniform spherical electron cloud with the bulk density.[15] This approach has been applied by Selby *et al.*[6] for sodium clusters.

Measurements on clusters having a diameter smaller than 100 Å show a radius dependence of the resonance energy which is not predicted by the above models. In the case of very small particles (diameter typically smaller than 12 Å), the extension of the electronic wave function outside the ion core becomes important and affects the plasmon frequency. The static polarizability (which is a measure of the volume occupied by the electrons) is corrected by adding a so-called spillout distance (t) to the classical sphere radius. Whichever reasonable dielectric constant is used, introducing the spillout in the Mie model results in a redshift of the resonance energy when decreasing the cluster size.

The Mie-Drude-spillout three-axes model has been applied by Selby *et al.*[6] to explain their gas-phase sodium cluster measurements. The center frequencies of the plasmon peaks can be calculated as

$$\omega_i = \frac{\omega_p}{[1 + \epsilon_m (L_i^{-1} - 1)]^{1/2}} \times \left[\frac{N r_s^3}{(X_0 + t)(Y_0 + t)(Z_0 + t)} \right]^{1/2} \ . \tag{7}$$

In order to interpret our results and the experimental data of Charlé, Schulze, and Winter, we have adopted a model based on the main physical idea that the dielectric constants near the surface and in the interior volume of the cluster are different. We next study the classical response of a coated sphere in which the interior ($r < R - d$) is characterized by the bulk dielectric function (ϵ_1) and the outer region ($R - d < r < R + t$) by the Drude dielectric function (ϵ_2). The parameters d and t (spillout) are chosen to be independent of the particle size. Under these hypotheses, the extension of Eq. (1) can be written as[28]

$$\sigma(\omega) = 9V \frac{\omega}{c} \epsilon_m^{1/2} \operatorname{Im} \left\{ \frac{(\epsilon_2 - \epsilon_m)(\epsilon_1 + 2\epsilon_2) + f(\epsilon_1 - \epsilon_2)(\epsilon_m + 2\epsilon_2)}{(\epsilon_2 + 2\epsilon_m)(\epsilon_1 + 2\epsilon_2) - f(\epsilon_1 - \epsilon_2)(2\epsilon_m - 2\epsilon_2)} \right\} \ , \tag{8}$$

where f is the ratio of the interior to the total volume, $f=\{(R-d)/(R+t)\}^3$.

V. DISCUSSION

A. Matrix effects

In order to discuss the absorption features of silver clusters it is important to distinguish between the matrix effects and the intrinsic particle response. Unfortunately at present no gas-phase data are available for small neutral silver clusters. In order to ascertain the matrix effect, we have measured the optical absorption of Ag_7, Ag_{11}, Ag_{15}, and Ag_{21} in solid krypton and xenon (deposition energy 30 eV). For each size, the number of particles contained in those matrices was two or three times smaller than the number of clusters embedded in solid argon. These spectra are presented in Fig. 5 together with the argon matrix results.

Except for Ag_{11} where it is less evident, the basic structures of the spectra are well reproduced when changing the matrix gas. These data also clearly show that the fragmentation increases as Ar→Kr→Xe, as can be seen in the spectra which exhibit atomic features. The monomer signal is strongest in the case of Ag_7 and Ag_{11} in xenon (peaks at 3.87, 3.8, and 3.71 eV) but it can also be seen for Ag_7 and Ag_{15} in krypton (at 4.03, 3.96, and 3.85 eV). It should be noted that the fragmentation decreases when increasing the cluster size. This is not obvious from the spectra since the vertical scales were chosen to emphasize the shapes, and not to compare the relative intensities. The Ag_{11}/Xe spectrum is the only case which clearly shows the dimer absorption (centered at 4.35 and 3.19 eV) while excitation spectroscopy detects Ag_2 in every sample.

In Fig. 6 we plot the energy shifts between Xe→Kr and between Xe→Ar for the main absorption peaks of each cluster size studied. We observe that the energy shifts caused by changing the matrix gas are relatively independent of the cluster size. A linear fit gives the energy shifts 0.13 eV (Xe→Kr) and 0.22 eV (Xe→Ar). Accordingly, it may be assumed that the plasmon frequencies observed in rare-gas matrices are related to the corresponding gas-phase value by a constant energy shift, at least for the sizes considered here.

The Mie condition [Eq. (2)] is well verified by several measurements done in rare-gas matrices. For example, Welker and Martin[3] observed the absorption of sodium atom vapor cocondensed with xenon on a transparent substrate. At a sodium concentration of 5%, where we expect large particles to form, the spectra are composed of a single broad absorption band centered at 2.4 eV. This energy is in good agreement with Eq. (2), using $\epsilon_m=2.31$ (i.e., the value for bulk xenon),[30] and the experimental $\epsilon(\omega)$ value of bulk sodium.[31] In addition Charlé, Schulze, and Winter[20] find the absorption peak of silver particles having a mean diameter of 100 Å in argon matrices to be 3.26 eV, which verifies the classical relation, using $\epsilon_m=1.7$ (i.e., the ϵ value of bulk argon) (Ref. 30) and the experimental dielectric constant of bulk silver.[31] The plasmon peak of the same particle in the gas phase is obtained using the Mie condition and introducing $\epsilon_m=1$.

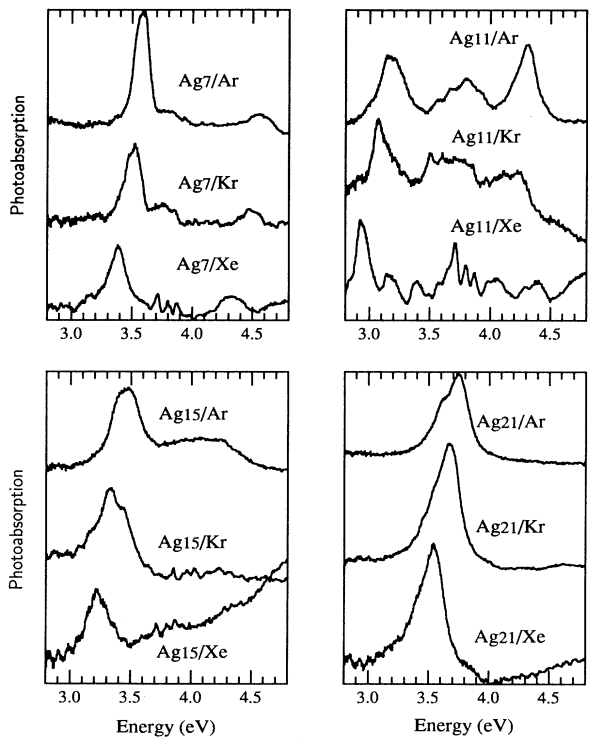

FIG. 5. Photoabsorption spectra of silver clusters for sizes $N=7$, 11, 15, and 21 embedded in argon, krypton, and xenon matrices. In order to reveal the structure of the spectra, the vertical scales are arbitrary. The triple narrow peak structure visible in several spectra is an atomic feature due to the fragmentation. The dimer absorption bands are only visible in the Ag_{11}/Xe spectrum at 3.19 and 4.35 eV. They are also due to fragmentation.

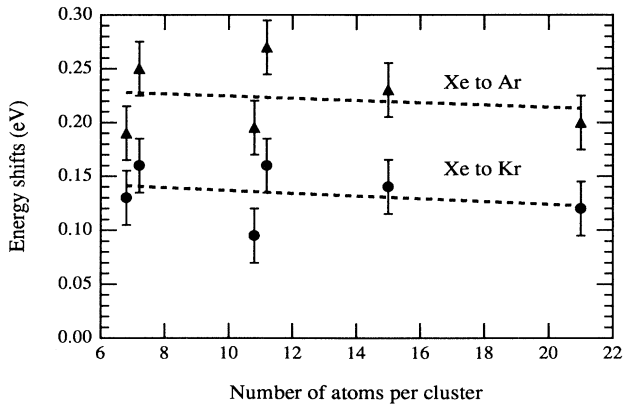

FIG. 6. Energy shifts of the Ag_N absorption peaks ($N=7$, 11, 15, and 21) due to the change of the matrix gas from xenon to krypton (points) and from xenon to argon (triangles) vs cluster size. For the heptamer the two peaks are used. In the case of Ag_{11} we have omitted the intermediary peak because its position is not clear for the deposition in xenon (see Fig. 5). The dashed lines are linear fits.

For silver clusters we find an energy of 3.50 eV, which indicates that the argon matrix causes a redshift of 0.24 eV. In the same way we calculate redshifts of 0.32 and 0.42 eV with respect to the gas-phase energy for particles, respectively, in krypton ($\epsilon_{Kr}=1.95$) (Ref. 30) and xenon matrices. This implies shifts of 0.1 and 0.18 eV, respectively, when changing the matrix gas Xe→Kr and Xe→Ar, which is similar to the values obtained from our measurements (0.13 and 0.22 eV).

We conclude from this discussion that for a given matrix, the relative position of the spectra corresponding to different sizes is an intrinsic feature of the clusters. Also the observed peak structures and peak widths are independent of the matrix.

B. Size effects on the plasmon energy

In order to compare the absorption energies obtained in our samples with the experimental data known for bigger silver clusters in solid argon (Charlé, Schulze, and Winter[20]), we have chosen to present in Fig. 7 the mean absorption energy $\langle \hbar\omega \rangle$ of each particle size, as defined in Sec. III (see Table I). Our measurements show for all sizes a redshift of the mean absorption energy with respect to the extrapolation of bigger clusters. In addition the mean adsorption energies present a pronounced oscillation with two maxima at $N=8$ and 18.

The optical absorption of small silver clusters is related to several physical effects, and only a dynamic calculation, taking into account the geometrical structure of the clusters and the contribution of the d and s conduction electrons to the absorption energies, can fully explain the observed spectra. We adopt the point of view that the observed spectra reflect a collective excitation of the electrons, and that we can use the Mie theory in relation with simple models to interpret our data.

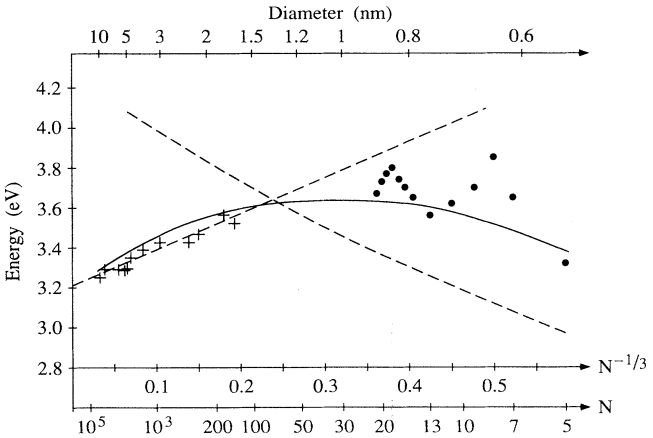

FIG. 7. Comparison of the mean absorption energies between the very small particle results (our measurements) and the results for bigger particles [Charlé, Schulze, and Winter (Ref. 20)], respectively, marked with points and crosses. The dashed line is a linear fit of the measurements of Charlé, Schulze, and Winter and the dashed curve corresponds to the calculation of spherical clusters using a spillout of 0.75 Å in the Mie-Drude-spillout model. The results obtained from the coated spherical model correspond to the continuous curve, using $d=2.8$ Å and a spillout of 0.45 Å (see the text).

It has been shown in the case of sodium clusters[6] that the absorption energies as a function of size can be understood by introducing a spillout of the conduction electrons. In the case of Ag clusters another important effect is the evolution of the relative contributions of the s and d electrons as a function of size. It has already been mentioned that the effect of the interband transitions due to the d electrons is essential to understand the experimental plasmon resonance in bulk silver. It is also important for large particles (diameter ≈ 100 Å) as the results of Charlé, Schulze, and Winter[20] indicate, because the measured plasmon resonance can only be explained if the bulk dielectric constant is introduced in the Mie condition [Eq. (2)]. The situation may be different for smaller particles, where the effect of the surface atoms is large.

In order to gain a first understanding of the importance of the s-d contribution in small clusters, we have calculated in the local-spin-density approximation, using a Gaussian basis reproducing well the 4d, 5s, and 5p atomic orbitals,[32] the geometrical and electronic structure of a heptamer having the shape of a pentagonal bipyramid. A pseudopotential was used in which the 4d and 5s electrons are considered as valence electrons. The optical transitions were calculated in a non-self-consistent way, in assuming that the Slater determinants built from the Kohn-Sham one-electron wave functions give a reasonable approximation for the determination of the dipolar matrix elements. The results clearly indicate the presence of a main absorption peak situated at 2.6 eV (experimental value 3.6 eV) and smaller amplitude resonances at larger energies. It is known that the local-density approximation does not predict correctly the energies of the excited states; the important point is, however, that the d contribution to the transitions contributing to the main peak is very weak. Some transitions are dominated by the d contribution, but they occur at larger energies (around 6 eV or more). It is also interesting to note that the decomposition of the one-electron wave functions in spherical harmonics around the center of the cluster clearly reveals a shell-type structure, which is important in determining the cross sections associated with the different transitions. Although this calculation is still preliminary, it indicates that the observed transitions in small clusters are dominated by s-p contributions. In a simple model, this can be taken into account in assuming that the dielectric constant of small clusters is of Drude type, and keeping only 5s valence electrons.

We show in Fig. 7 (dashed curve) the resonance frequencies obtained in the Mie-Drude-spillout model (see Sec. IV) applied to silver spherical-like particles in argon with the bulk electronic density. For sodium clusters, the spillout t was deduced from the experimental data of the static polarizability. Such measurements are not available for Ag particles, and we interpolate the spillout calculated for metal surfaces by Lang and Kohn[33] at various electron densities. We obtain $t=0.75$ Å for silver. On the basis of a self-consistent calculation for the polarizability of jellium spheres done by Puska, Nieminen, and Manninen,[34] we find $t=0.6$ Å. The value $t=0.75$ Å has

been chosen in Fig. 7. We see that the calculated plasmon resonance frequencies are shifted on the average by only 0.4 eV towards the red, also the model overestimates the redshift of the smaller clusters. An important point of this simple model is that it does not explain the size dependence of the plasmon energies for the larger clusters. Also the matrix shifts calculated within the Drude model are overestimated with respect to the measurements.

In order to describe in a phenomenological way the evolution of the average position as a function of size, we have calculated the absorption of a coated sphere [see Eq. (8)]. Although this model is certainly approximate, it has the advantage that it takes into account the increasing contribution of the d electrons when the size increases. We assume that the outer layer, of width $(d+t)$, is described by a Drude dielectric constant and that the inner sphere, of radius $(R-d)$, is described by the bulk dielectric constant. We display in Fig. 7 (continuous curve) the results obtained using a spillout $t=0.45$ Å and $d=2.8$ Å. Good agreement is found with the experimental results for the entire size range; in particular, the large-particle resonance frequencies are well reproduced. Changing the spillout to $t=0.75$ Å emphasizes the redshift of the resonance frequencies, but retains the same general behavior.

In the case of a Drude model and for a cluster of ellipsoidal shape, the average frequency $\langle\omega\rangle$ is proportional to $(1/\alpha)^{1/2}$ where α is the average polarizability per atom, if we assume that the width of the total spectrum is small compared to the center frequency. It is thus tempting to interpret the oscillations of the plasma energies, which clearly appear in Fig. 7, as an oscillation of the polarizability per atom. α goes through a minimum when the plasmon energy is maximum. Indeed the experimental average polarizabilities of Na_n and K_n (Ref. 35) clusters show a distinct minimum for the closed-shell clusters ($n=2,8$), and it drops again when the region of the next closed-shell clusters ($n=18,20$) is reached. The same behavior is confirmed by the calculation of Puska, Nieminen, and Manninen[34] for Li and Al particles. Furthermore the order of magnitude of the change of $\langle\hbar\omega\rangle$ between Ag_{18} and Ag_{13} (equal to 0.8) is of the right order when compared with the Na experimental polarizability. These data thus suggest that the shell structure in silver clusters is an effect which has to be introduced to explain the average position of the plasmon resonance absorption.

C. Multipeak structure of the spectra

The absorption spectra presented in Fig. 3 may be separated in two groups. In the first one (Ag_2 to Ag_{11}) the spectra look very different from each other, while the spectra of the second group (Ag_{13} to Ag_{21}) show a regular evolution. They consist of a strong peak in the red plus a less intense absorption band in the blue, with the exception of Ag_{21}. The common feature of all spectra is, however, that they show a multipeak structure (see also Table I).

In the Mie theory, as the resonance condition given in Eq. (5) indicates, the multipeak structure of the absorption spectra is related to the particle shape, via the effect of depolarization. For the alkali-metal clusters, which are well described by a shell model, the shape depends mainly on the number of valence electrons. Closed-shell clusters are spheres, while open-shell ones are approximated by ellipsoidal shapes. In the Nilsson-Clemenger model,[15] which takes into account the shape effect in a particularly simple way, the resonance frequencies are expressed by Eq. (7), if the spillout is also included. In Fig. 3 the calculated plasmon energies (black points), using Eq. (7) and $t=0.75$ Å, are compared with the absorption spectra for each cluster size. Apart from a systematic redshift with respect to the experimental data, already seen in Fig. 7, the agreement between the calculated values and the measurements is surprisingly good. The total width D of the spectra is well reproduced, and the number and position of peaks agree well with the data. This is, as expected, particularly true for the larger-size clusters. The stronger exception is Ag_5, in which three well-separated peaks are predicted, while we observe only two absorption bands. The Ag_8 spectrum also shows a small absorption in the red (3.16 eV), which is not predicted by the model; a similar behavior was observed for Na_8.[8] The Ag_{20} spectrum has a strongly asymmetric main line shape plus a smaller shoulder on the blue side. As calculations of Yannouleas *et al.*[36] have suggested for sodium, these features are possibly caused by the fragmentation of the plasmon due to the coupling with a single particle excitation. The relative intensity of the peaks is in qualitative agreement with the predicted peak intensity ratio (1:1:1 or 1:2), see, e.g., the inversion of the intensity ratio for Ag_{19} and Ag_{21}.

We conclude from this analysis that the simple shell model proposed by Clemenger[15] reproduces fairly well the main structure of the observed spectra and especially for the larger-size clusters. A detailed analysis of the measured spectra cannot, however, be expected by this model and has to await more sophisticated calculations such as RPA or CI. Notice also that this agreement confirms the hypothesis that the participation of the d electrons in the observed transitions is weak for small clusters.

D. Width of the electronic excitations

The typical measured linewidth of the absorption peaks for small silver clusters in a rare-gas matrix is 0.2 eV (Table I). The value of the plasmon width is practically constant when changing the matrix rare gas (Fig. 5). In addition the annealing of the sample up to 25 K for argon and 35 K for xenon does not modify the characteristic features of the absorption spectra (peak intensities and linewidths). Whereas the plasmon resonance frequency is mainly a function of the equilibrium properties of the cluster, its width is determined by processes such as shape fluctuations, Landau damping (the decay of the collective excitation into single-particle excitation), and

electron-phonon scattering (the decay of the electronic excitation into heat). In addition, the cluster-matrix interaction can also contribute to the linewidth.

For silver particles greater than 150 atoms, the measurements of Charlé, Schulze, and Winter[20] show that the total width of the plasmon peak scales with the inverse of the cluster diameter. If we extrapolate this behavior to the size range of our data, we get a linewidth which is comparable to the largest total width (D) of our absorption features. This is certainly due to the fact that their linewidth is the sum of several individual plasmon absorption lines, belonging to clusters of different sizes. The gas-phase measurements of Tiggesbäumker *et al.*[21] present linewidths of 0.6 eV, which are not comparable with those of supported clusters at 10 K because the particles were produced by sputtering and were accordingly very hot ($T=1000$ K or more).

The width arising from adiabatic thermal fluctuations of the cluster shape was calculated for alkali-metal clusters in different ways[37,38] which are not valid at low temperature, because they principally do not take into account the zero-point fluctuation. In fact, calculations of Penzar, Ekardt, and Rubio[39] or Pacheco, Broglia, and Mottelson[40] show that the zero-point-motion effect becomes non-negligible below 300 K and yields a finite linewidth already at $T=0$ K, which was estimated to be around 70 meV in the case of Na_{10}. It is more difficult to get an idea of how much the "Landau damping" affects the linewidth. Jellium model calculations[41] of spherical sodium clusters show that the electron-hole excitations produce some small fine structures in the imaginary part of $\alpha(\omega)$ and a broadening of the plasmon lines, which is important for Na_{198} but becomes negligible for Na_{20}. Finally Dam and Saunders[42] estimate that the magnitude of the contribution from the electron-phonon interaction to the plasmon width is of the order of the thermal energy; this effect is thus negligible at our matrix temperatures. Assuming that these predictions are valid for silver clusters, we conclude that in the case of very small particles at 10 K the main phenomenon which broadens the plasmon line is the zero-point fluctuation, which causes a linewidth of typically 0.1 eV. Another origin of the observed linewidth must certainly be found in the cluster-matrix interaction.

The conservation of the same absorption spectrum during and after the annealing of the sample indicates that for the sizes studied all cluster positions in the matrix are probably equivalent (which is not the case for the atom[43]). Also the independence of the linewidth with respect to the rare gas forming the matrix confirms that it is intrinsically due to the particle. Another cause of line broadening could be related to the presence of different isomers in the matrix, although there are no clear signs to support this idea.

VI. SUMMARY AND CONCLUSIONS

We have obtained well-resolved optical-absorption spectra of small size-selected Ag_n ($n=2-21$) clusters embedded in argon matrices, in the energy range 2.1–6.2 eV. Except for Ag_2 and Ag_3, the spectra are principally formed by one, two, or three strong absorption peaks at energies situated between 3 and 4.5 eV.

Measurements on Ag_n ($n=7$, 11, 15, and 21) in krypton and xenon matrices indicate that the medium does not modify the shape of the spectra. The main matrix effect on the absorption features is a redshift with respect to the gas-phase spectra, which is practically independent of the cluster size in the size range measured. This redshift is estimated to be 0.24 eV for an argon matrix.

A classical study (Mie theory) introducing a spillout and using a Drude dielectric constant for the cluster gives satisfactory agreement concerning the main features of the observed spectra. In this model, the strong absorption bands are understood as a collective excitation of the s electrons and the one- to three-peak structure is a consequence of the ellipsoidal shape of the cluster. The integrated intensity corresponds on the average to 88% of the total oscillator strength if we take into account only s electrons. This proportion is the same for all clusters. The mean absorption energies are redshifted with respect to earlier predictions based on bigger-sized clusters. The model attributes this shift to the importance taken by the spillout in the very small clusters, which induces a decrease of the electron density and consequently reduces the resonance energy. More precisely the behavior of the mean absorption energies along the size range shows an oscillation with two maxima at $N=8$ and 18, which can be explained as an s-electron shell structure effect.

The fact that the majority of phenomena observed can be explained involving only s electrons is a strong indication that very small silver clusters possess alkali-metal-like electronic properties. However, it is clear that this suggestion must be confirmed by calculations which take explicitly into account the effect of the d electrons and the geometrical structure of the particle. Also the high resolution of the spectra reveals fine structures which cannot be explained in a simple model. Work is in progress in order to increase the size of the clusters studied.

ACKNOWLEDGMENTS

The authors wish to express their thanks for helpful discussions with W. de Heer, F. Reuse, and N. Dam. F. Reuse has in particular calculated the s-d contribution to the optical transitions in the heptamer silver cluster. This work has been supported by the Swiss National fund, Contract No. 20-28913.90.

[1]U. Kreibig and L. Genzel, Surf. Sci. **156**, 678 (1985).
[2]U. Kreibig and C. von Fragstein, Z. Phys. **224**, 307 (1969).
[3]T. Welker and T. P. Martin, J. Chem. Phys. **70**, 5683 (1979).
[4]H. Abe, K. P. Charlé, B. Tesche, and W. Schulze, Chem. Phys. **68**, 137 (1982).
[5]G. Mie, Ann. Phys. (Leipzig) **25**, 377 (1908).
[6]W. A. de Heer, K. Selby, V. Kresin, J. Masui, M. Vollmer, A. Châtelain, and W. D. Knight, Phys. Rev. Lett. **59**, 1805

(1987); K. Selby, M. Vollmer, J. Masui, V. Kresin, W. A. de Heer, and W. D. Knight, Phys. Rev. B **40**, 5417 (1989); K. Selby, V. Kresin, J. Masui, M. Vollmer, W. A. de Heer, A. Scheidemann, and W. D. Knight, *ibid.* **43**, 4565 (1991).

[7]V. Bonačić-Koutecký, J. Pittner, C. Scheuch, M. F. Guest, and J. Koutecky, J. Chem. Phys. **96**, 7938 (1992).

[8]S. Pollack, C. R. C. Wang, and M. M. Kappes, J. Chem. Phys. **94**, 2496 (1991); C. R. C. Wang, S. Pollack, and M. M. Kappes, Chem. Phys. Lett. **166**, 26 (1990).

[9]J. Blanc, M. Broyer, J. Chevaleyre, Ph. Dugourd, H. Kühling, P. Labastie, M. Ulbricht, J. P. Wolf, and L. Wöste, Z. Phys. D **19**, 7 (1991).

[10]C. Bréchignac, P. Cahuzac, F. Carlier, and J. Leygnier, Chem. Phys. Lett. **164**, 433 (1989).

[11]N. Dam and W. A. Saunders, Z. Phys. D **19**, 85 (1991).

[12]H. Fallgren and T. P. Martin, Chem. Phys. Lett. **168**, 233 (1990).

[13]C. Bréchignac, Ph. Cahuzac, N. Kebaili, J. Leygnier, and A. Sarfati, Phys. Rev. Lett. **68**, 3916 (1992).

[14]J. Blanc, V. Bonačić-Koutecký, M. Broyer, J. Chevaleyre, Ph. Dugourd, J. Koutecký, C. Scheuch, J. P. Wolf, and L. Wöste, J. Chem. Phys. **96**, 1793 (1992).

[15]K. Clemenger, Phys. Rev. B **32**, 1359 (1985); Ph.D. thesis, University of California, Berkeley, 1985.

[16]W. Ekardt and Z. Penzar, Phys. Rev. B **43**, 1322 (1991).

[17]S. Saito, G. F. Bertsch, and D. Tomànek, Phys. Rev. B **43**, 6804 (1991).

[18]V. Kresin, Phys. Rev. B **45**, 14 321 (1992).

[19]V. Bonačić-Koutecký, P. Fantucci, and J. Koutecký, J. Chem. Phys. **93**, 3802 (1990); Ph. Dugourd, J. Blanc, V. Bonačić-Koutecký, M. Broyer, J. Chevaleyre, J. Koutecký, J. Pittner, J. P. Wolf, and L. Wöste, Phys. Rev. Lett. **67**, 2638 (1991).

[20]K. P. Charlé, W. Schulze, and B. Winter, Z. Phys. D **12**, 471 (1989).

[21]J. J. Tiggesbäumker, L. Köller, H. O. Lutz, and K. H. Meiwes-Broer, Chem. Phys. Lett. **190**, 42 (1992); in *From Clusters to Crystals,* edited by P. Jena, S. N. Khanna, and B. K. Rao (Kluwer, Boston, 1992), Vol. II, p. 1001.

[22]K. H. Meiwes-Brower (private communication).

[23]W. Harbich, S. Fedrigo, F. Meyer, D. M. Lindsay, J. Lignieres, J. C. Rivoal, and D. Kreisle, J. Chem. Phys. **93**, 8535 (1990).

[24]H. Abe, W. Schultze, and B. Tesche, Chem. Phys. **47**, 95 (1980); S. A. Mitchell and G. A. Ozin, J. Phys. Chem. **88**, 1425 (1984).

[25]S. Fedrigo, W. Harbich, and J. Buttet (unpublished).

[26]W. Harbich, S. Fedrigo, and J. Buttet, Chem. Phys. Lett. **195**, 613 (1992).

[27]D. M. Lindsay, F. Meyer, and W. Harbich, Z. Phys. D **12**, 15 (1989).

[28]In the case of particles in a medium,

$$C=\left\{\left[\frac{E_{\rm loc}}{\langle E\rangle}\right]^2\frac{1}{n}\right\}\frac{\pi e^2}{2\epsilon_0 m_e c},$$

where $E_{\rm loc}$ is the local electric field, $\langle E\rangle$ is the macroscopic field, and n is the refractive index [see J. D. Jackson, *Classical Electrodynamics* (Wiley, New York, 1975) and B. di Bartolo, *Optical Interactions in Solids* (Wiley, New York, 1968)]. In our case, $E_{\rm loc}$ is unknown and we suppose that $E_{\rm loc}/\langle E\rangle=1$.

[29]See, for example, C. F. Bohren and D. R. Huffman, *Absorption and Scattering of Light by Small Particles* (Wiley, New York, 1983).

[30]M. L. Klein and J. A. Venables, *Rare Gas Solids* (Academic, New York, 1977), Vol. II.

[31]E. D. Palik, *Handbook of Optical Constants of Solids* (Academic, New York, 1985), Vol. I; *ibid.* (Academic, New York, 1991), Vol. II.

[32]For a detailed description of the numerical procedures, see, e.g., F. Reuse, S. N. Khanna, V. de Coulon, and J. Buttet, Phys. Rev. B **41**, 11 743 (1990).

[33]N. D. Lang and W. Kohn, Phys. Rev. B **1**, 4555 (1970); **7**, 3541 (1973).

[34]M. J. Puska, R. M. Nieminen, and M. Manninen, Phys. Rev. B **31**, 3487 (1985).

[35]W. D. Knight, K. Clemenger, W. A. de Heer, and W. A. Saunders, Phys. Rev. B **31**, 2539 (1985).

[36]C. Yannouleas, R. A. Broglia, M. Brack, and P. F. Bortignon, Phys. Rev. Lett. **63**, 255 (1989).

[37]J. M. Pacheco and R. A. Broglia, Phys. Rev. Lett. **62**, 1400 (1989).

[38]G. F. Bertsch and D. Tománek, Phys. Rev. B **40**, 2749 (1989).

[39]Z. Penzar, W. Ekardt, and A. Rubio, Phys. Rev. B **42**, 5040 (1990).

[40]J. M. Pacheco, R. A. Broglia, and B. R. Mottelson, Z. Phys. D **21**, 289 (1991).

[41]W. Ekardt, Phys. Rev. B **31**, 6360 (1985).

[42]N. Dam and W. A. Saunders, Phys. Rev. B **46**, 4205 (1992).

[43]S. A. Mitchell, J. Farrell, G. A. Kenney-Wallace, and G. A. Ozin, J. Am. Chem. Soc. **102**, 7702 (1980).